# Bulk and Shear Mechanical Loss of Titania-doped Tantala

Matthew Abernathy<sup>a,\*</sup>, Gregory Harry<sup>1</sup>, Jonathan Newport<sup>1</sup>, Hannah Fair<sup>1</sup>, Maya Kinley-Hanlon<sup>1</sup>, Samuel Hickey<sup>1</sup>, Isaac Jiffar<sup>1</sup>, Cairo Thompson<sup>1</sup>, Andri Gretarsson<sup>c</sup>, Steve Penn<sup>d</sup>, Riccardo Basiri<sup>e</sup>, Eric Gustafson<sup>f</sup>, Iain Martin<sup>1</sup>

<sup>a</sup>NRC Research Associate, Naval Research Laboratory, Washington DC, 20375

<sup>b</sup>Physics Department, American University, Washington DC, 20016

<sup>c</sup>Department of Physics, Embry-Riddle Aeronautical University, Prescott AZ, 86301

<sup>d</sup>Hobart and William Smith Colleges, Geneva NY 14456

<sup>e</sup>Stanford University, Stanford CA 94305

<sup>f</sup>LIGO Laboratory, California Institute of Technology, Pasadena CA 91125

<sup>g</sup>Institute for Gravitational Research, Kelvin Building, University Avenue, Glasgow, G12

8QQ, Scotland, United Kingdom

### Abstract

We report on the mechanical loss from bulk and shear stresses in thin film, ion beam deposited, titania-doped tantala. The numerical values of these mechanical losses are necessary to fully calculate the Brownian thermal noise in precision optical cavities, including interferometric gravitational wave detectors like LIGO. We found the values from measuring the normal mode Q's, in the frequency range of about 2000-10,000 Hz, of silica disks coated with titania-doped tantala coupled with calculating the elastic energy in shear and bulk stresses in the coating using a finite element model. We fit the results to both a frequency independent and frequency dependent model and find  $\phi_{\text{bulk}} = (8.4 \pm 0.3) \times 10^{-5}, \ \phi_{\text{shear}} = (7.8 \pm 0.7) \times 10^{-5}$  with a frequency independent model and  $\phi_{\text{bulk}}(f) = (1.3 \pm 0.2) \times 10^{-4} - (9.8 \pm 4.7) \times 10^{-9} f$ ,  $\phi_{\text{shear}}(f) = (5.2 \pm 1.1) \times 10^{-5} + (5.4 \pm 2.1) \times 10^{-9} f$  with a frequency dependent (linear) model. The ratio of these values suggest that modest improvement in the coating thermal noise may be possible in future gravitational wave detector optics made with titania-doped tantala as the high index coating material by optimizing the coating design to take advantage of the two different mechanical loss angles.

#### 1. Introduction

Brownian thermal noise is one of the fundamental limiting noise sources in precision optical cavities [1, 2, 3]. This will be the case for the Advanced LIGO gravitational wave detectors when they reach their design sensitivity [4, 5]. The

 $<sup>{\</sup>rm *Corresponding\ author,\ matthew.abernathy.ctr@nrl.navy.mil}$ 

Advanced LIGO detectors are large, Michelson interferometers with Fabry-Perot cavity arms which are sensitive to astrophysical gravitational waves [6]. They began operation in fall of 2015 and successfully detected gravitational waves from the coalescence of binary black holes [7, 8]. The optical coatings [9] on the test masses of these interferometers are composed of alternating layers of ion beam sputtered (IBS) amorphous silica (SiO<sub>2</sub>) and titania-doped tantala (TiO<sub>2</sub>-doped  $Ta_2O_5$ ) [10]. Once commissioning is completed on the Advanced LIGO detectors around 2019 [5], the Brownian thermal noise [11] of these coatings is expected to limit the detectors observational capability at their most sensitive frequency range of 40-150 Hz. Coating thermal noise is expected to be a limiting noise source in future gravitational wave detectors as well [12].

Previous work on coating thermal noise [13, 14, 15] utilized the Levin approach [16] to the Fluctuation-Dissipation Theorem [17] for calculating the thermal fluctuations of the average cavity length from the mechanical loss of the coating materials. This work used a single mechanical loss angle  $\phi$  for each amorphous material, silica and titania-doped tantala. Following this, two mechanical loss parameters for the coating as a whole were constructed, averaged over the two amorphous materials. Each parameter was associated with a different direction of mechanical stresses of the coating as a whole:  $\phi_{\parallel}$  for stress parallel to the coating surface, and  $\phi_{\perp}$  for stress perpendicular to the coating surface [13].

A recent paper by Hong et al. [18] showed that because each of the amorphous materials used in the LIGO coating is described by two independent elastic constants (Young's modulus and Poisson's ratio, for example) there are two sources of uncorrelated thermal noise in each coating material. The imaginary components of these elastic constants are independent loss angles that give rise to separate uncorrelated thermal noises. Hong et al. suggested that loss angles based on bulk and shear stresses of each material be used for thermal noise calculations. Additionally, they showed the ratio of these two parameters can impact the expected thermal noise in the LIGO detectors by as much as 30%.

Modeling coating thermal noise with a single loss angle for each material creates similar uncertainty in the thermal noise of precision optical measurements other than gravitational wave detectors. Low noise optical stabilization cavities are used in producing narrow-linewidth laser frequency standards in optical atomic clocks [19], tests of fundamental physics [20], and precision spectroscopy [21]. In these fields, the measurement sensitivity is often limited by the linewidth of the stabilized laser, which in turn can be limited by the coating thermal noise within the optical stabilization cavity [22, 23]. Efforts to understand the molecular level causes of thermal noise [24, 25] and to model this loss [26] will also benefit from a complete characterization of all loss angles.

To address these issues we have measured both the bulk and shear mechanical losses of an ion beam sputtered titania-doped tantala coating. In Sections 2, 3.1, and 4 we give the methods of measurement, modeling, and analysis of the coating samples. Finally, in Section 4, we describe how these results impact the predicted thermal noise limits on the sensitivity of Advanced LIGO detectors and other precision measurement devices.

### 2. Measurements

The Fluctuation Dissipation Theorem [17] relates thermal noise to energy loss in a system [16]. We determined the energy loss in a mechanical system composed of a coating on a substrate by measuring the quality factor, Q, of the sample's elastic normal modes. The sample was a three inch (76 mm) diameter, 0.1 inch (2.5 mm) thick fused silica disk coated on one side with tantala doped with 25% titania as a cation percentage. The coating was deposited using ion beam deposition [27] at 50° Celsius over 5 hours by the Commonwealth Scientific and Industrial Research Organization (CSIRO) [28]. There was no post deposition annealing done with the sample.

The thickness of the coating was found by measuring, at both normal and 45 degree incidence, the transmission spectrum of the sample in the near infrared (528-1001 nm). The resulting spectra were then fit to the expected transmissivity at each angle of incidence with the spectra for normal incidence shown in Figure 2. The expected transmissivity was obtained by using the transfermatrix method [29]. A coating index of 2.119 for 25% titania-tantala (from [10]) was used while the fused silica substrate index was assumed to be 1.460 [30]. The thickness of the coating was found to be  $524\pm1$  nm. The error is dominated by systematics as can be seen in Figure 2.

To make modal Q measurements we suspended the coated silica disk in a vacuum of at least  $10^{-5}$  torr via a monolithic silica suspension, see [9, 10, 13]. The normal modes were excited using a comb capacitor situated near the sample. The stress versus time in the sample was then measured using a birefringence readout, see [9, 10, 13]. This data was heterodyned to a lower frequency, about 0.3 Hz, using a lock-in amplifier and stored digitally. The exponential decay times,  $\tau$ , of the normal modes were fit for directly. The quality factors, Q, of the modes were found from

$$Q(f_0) = \pi \tau f_0, \tag{1}$$

where  $f_0$  is the normal mode frequency. Results are shown in Table 1.

The Young's modulus of the coating was needed for the finite element modeling (see Section 3.1) and was measured using nanoindentation. Modulus values for indents at multiple locations and multiple depths were extracted using the method of Oliver and Pharr [31, 32], and the film modulus was extracted from the combined film/substrate moduli using the method of Song and Pharr [33]. The Young's modulus for the titania-tantala coating was measured to be  $162 \pm 5$  (systematic)  $\pm 11$  (statistical) GPa. The systematic uncertainty stems from the uncertainty in the Poisson ratio, assumed to be  $0.27 \pm 0.05$ . The statistical uncertainty stems from the uncertainty in the fit using the Song and Pharr model.

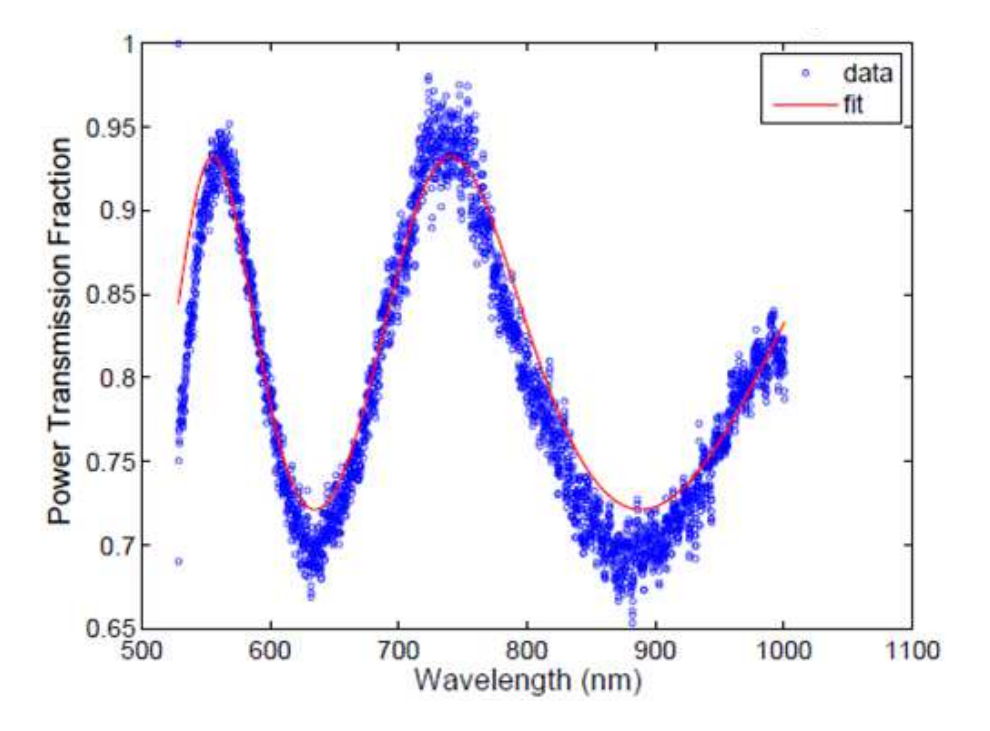


Figure 1: Optical power (shown as circular data points) transmitted by the titania doped tantala coating from a beam normal to the surface as a function of effective wavelength, along with a fit to a model (shown as thin curve) with a coating thickness of 524  $\mu$ m, substrate index  $n_{\rm sub} = 1.460$ , and coating index  $n_{\rm coat} = 2.119$ .

## 3. Analysis

The mechanical loss for titania doped tantala in shear and bulk deformation,  $\phi_{\rm shear}$  and  $\phi_{\rm bulk}$ , are related to the measured modal Q values through

$$1/Q_{1} = \frac{E_{\text{shear},1}}{E_{\text{tot},1}} \phi_{\text{shear}}(f_{1}) + \frac{E_{\text{bulk},1}}{E_{\text{tot},1}} \phi_{\text{bulk}}(f_{1}) + \phi_{\text{silica}}(f_{1}),$$

$$1/Q_{2} = \frac{E_{\text{shear},2}}{E_{\text{tot},2}} \phi_{\text{shear}}(f_{2}) + \frac{E_{\text{bulk},2}}{E_{\text{tot},2}} \phi_{\text{bulk}}(f_{1}) + \phi_{\text{silica}}(f_{2}),$$

$$\vdots$$

$$1/Q_{n} = \frac{E_{\text{shear},n}}{E_{\text{tot},n}} \phi_{\text{shear}}(f_{n}) + \frac{E_{\text{bulk},n}}{E_{\text{tot},n}} \phi_{\text{bulk}}(f_{n}) + \phi_{\text{silica}}(f_{n}).$$

Here n is the total number of normal modes measured,  $Q_i$  is the i<sup>th</sup> normal mode quality factor,  $E_{\rm shear,i}/E_{\rm tot,i}$  is the ratio of energy in shear deformation of the coating to the total elastic energy in the sample for the i<sup>th</sup> normal mode,  $E_{\rm bulk,i}/E_{\rm tot,i}$  is the ratio of energy in bulk deformation of the coating to the

Table 1: Modal Q's of eight modes of the titania-tantala coated silica disk. The Mode Number is a count starting from the lowest frequency mode (with degenerate modes not given a separate number). The Mode Number for the high frequency modes at 37013 and 41521 Hz comes from the Finite Element Model (see Section 3.1). The uncertainty in Q,  $\delta Q$ , is the uncertainty in the fit to an exponential ring down.

Mode			
Number	Frequency (Hz)	$Q \ (\times 10^{6})$	$\delta Q~(\times 10^6)$
1	2768	1.315	0.006
2	4183	1.015	0.001
3	6320	1.14	0.01
4	9668	0.98	0.02
5	10943	0.89	0.02
6	16615	1.05	0.01
14	37013	2.22	0.02
16	41521	1.82	0.03

total elastic energy in the sample for the i<sup>th</sup> normal mode, and  $\phi_{\text{silica}}(f_i)$  is the loss angle of the silica at the i<sup>th</sup> normal mode frequency.

### 3.1. Finite Element Model

We used the COMSOL Multiphysics finite element analysis program to calculate the shear and bulk energy in the coating as well as the total elastic energy in the sample. The model was composed of a substrate designed to match the geometry of the laboratory silica substrate with matching material parameters with a thin film defined by a thickness, t, the top surface of the substrate, and the material parameters of the film. The mesh size was determined by a single parameter, S, which limits the maximum element size in the film. Meshing was done by first applying a free triangular mesh to the surface of the film, with a minimum element size determined by S/10, which was swept through the film material onto the top surface of the substrate. This results in a film that was modeled by a single layer of triangular prism elements. A free tetrahedral mesh was then applied to the substrate using a maximum element size of  $10 \times S$ .

Modal frequencies and energy ratios were calculated using an eigenvalue solver to find the first 40 eigenmodes, the first 6 of which are zero-energy spatial modes. The resulting eignefrequencies show an exponential dependence on the value of S, which asymptotically approach a constant value for small values of S. The final value of S=0.001 m was chosen to give frequencies within 3% of the asymptotic values while still being calculable in reasonable times. The energy ratios were then calculated from

$$E_{\text{bulk}} = \int_{\text{coating}} \frac{K}{2} \Theta^2 dV, \tag{3}$$

$$E_{\text{shear}} = \int_{\text{coating}} \mu \Sigma_{ij} \Sigma_{ij} dV.$$
 (4)

Table 2: Material parameters of the titania-tantala coating used in the finite element analysis of elastic energy distribution.

Parameter	Value	Unit
Coating thickness, t	524	nanometer
Coating Young's modulus, $Y$	162	gigapascal
Coating Poisson ratio, $\sigma$	0.27[34]	-
Coating Density, $\rho$	5500[35]	kilogram/meter <sup>3</sup>
Coating bulk modulus, $K$	108	gigapascal
Coating shear modulus, $\mu$	65	gigapascal
Silica Young's Modulus, $Y_{\text{silica}}$	72.2	gigapascal
Silica Poisson ratio, $\sigma_{\rm silica}$	0.167	-
Silica Density, $\rho_{\rm silica}$	2200	kilogram/meter <sup>3</sup>
Silica bulk modulus, $K_{\rm silica}$	36.4	gigapascal
Silica shear modulus, $\mu_{\rm silica}$	31.1	gigapascal

$$E_{\text{tot}} = \int_{\text{substrate}} \left( \frac{K_{\text{silica}}}{2} \Theta^2 + \mu_{\text{silica}} \Sigma_{ij} \Sigma_{ij} \right) dV +$$
 (5)

$$\int_{\text{coating}} \left( \frac{K}{2} \Theta^2 + \mu \Sigma_{ij} \Sigma_{ij} \right) dV.$$
 (6)

Here  $\Theta$  and  $\Sigma_{ij}$  are the coating strain tensor's bulk and shear components[18], respectively, K is the coating bulk modulus,  $\mu$  is the coating shear modulus,  $K_{\rm silica}$  is the silica bulk modulus, and  $\mu_{\rm silica}$  is the silica shear modulus. The bulk and shear moduli are related to the Young's modulus, Y, and Poisson ratio,  $\sigma$ , by

$$K = \frac{Y}{3(1 - 2\sigma)} \tag{7}$$

$$\mu = \frac{Y}{2(1+\sigma)}.\tag{8}$$

The material and geometric parameters used in the finite element models are shown in Table 2 and the ratios of  $E_{\text{bulk}}$  and  $E_{\text{shear}}$  to the total elastic energy for each resonant mode measured,  $E_{\text{tot}}$ , are shown in Table 3.

Equations (2) are now a series of n equations with  $2 \times n$  unknowns, the  $\phi_{\text{shear}(f_i)}$  and  $\phi_{\text{bulk}(f)}$  with  $i \in (1, n)$ . This is an underconstrained system with no unique solution for  $\phi_{\text{shear}(f)}$  and  $\phi_{\text{bulk}(f)}$ .

To find a solution, we treat  $\phi_{\text{shear}}(f_i)$  and  $\phi_{\text{bulk}}(f_i)$  as constant for pairs of normal modes with nearby frequencies. This is not unreasonable as the mechanical loss of coating materials has been observed to have only a weak frequency dependence [36]. We then solve for  $\phi_{\text{shear}}(f_i)$  and  $\phi_{\text{bulk}}(f_i)$  at the average of the two normal mode frequencies from

$$\begin{pmatrix} 1/Q_i - \phi_{\text{silica}}(f_i) \\ 1/Q_{i+1} - \phi_{\text{silica}}(f_{i+1}) \end{pmatrix} = \mathbf{A} \cdot \begin{pmatrix} \phi_{\text{shear}}(f_a) \\ \phi_{\text{bulk}}(f_a) \end{pmatrix}$$
(9)

Table 3: Energy ratios for shear and bulk motion in the coating for all normal modes measured.

Mode		
Number	$E_{\rm shear}/E_{\rm tot} \times 10^4$	$E_{\rm bulk}/E_{\rm tot} \times 10^4$
1	1.04	0.666
2	8.49	4.84
3	10.1	1.03
4	8.98	3.63
5	9.86	1.26
6	9.43	2.38
14	9950	56
16	9130	870

Table 4: Values of  $\phi_{\text{shear}}(f_i)$  and  $\phi_{\text{bulk}}(f_i)$  with uncertainties for titania-doped tantala versus frequency.

Mode Numbers	Frequency $f_a$	$\phi_{\text{shear}}(f_a) + \delta\phi_{\text{shear}}(f_a)$	$\phi_{\text{bulk}}\left(f_{a}\right) + \delta\phi_{\text{bulk}}\left(f_{a}\right)$
1  and  2	$3476~\mathrm{Hz}$	$(6.7 \pm 0.2) \times 10^{-4}$	$(8.4 \pm 0.8) \times 10^{-4}$
2 and $3$	$5251~\mathrm{Hz}$	$(8.0 \pm 0.3) \times 10^{-4}$	$(6 \pm 1) \times 10^{-4}$
3 and $4$	$7994~\mathrm{Hz}$	$(7.8 \pm 0.4) \times 10^{-4}$	$(9 \pm 2) \times 10^{-4}$
4 and $5$	$10306~\mathrm{Hz}$	$(11.4 \pm 0.7) \times 10^{-4}$	$(-0.4 \pm 2) \times 10^{-4}$
5 and $6$	$13697~\mathrm{Hz}$	$(12 \pm 2) \times 10^{-4}$	$(-8 \pm 10) \times 10^{-4}$

where

$$\mathbf{A} = \begin{pmatrix} \frac{E_{\text{shear,i}}}{E_{\text{tot,i}}} & \frac{E_{\text{bulk,i}}}{E_{\text{tot,i}}} \\ \frac{E_{\text{shear,i+1}}}{E_{\text{tot,i+1}}} & \frac{E_{\text{bulk,i+1}}}{E_{\text{tot,i+1}}} \end{pmatrix}. \tag{10}$$

This can be rewritten in terms of the inverse matrix  $\mathbf{A}^{-1}$ 

$$\begin{pmatrix} \phi_{\text{shear}}(f_a) \\ \phi_{\text{bulk}}(f_a) \end{pmatrix} = \mathbf{A}^{-1} \cdot \begin{pmatrix} 1/Q_i - \phi_{\text{silica}}(f_i) \\ 1/Q_{i+1} - \phi_{\text{silica}}(f_{i+1}) \end{pmatrix}, \tag{11}$$

and  $f_a = (f_i + f_{i+1})/2$  is the average frequency of these two modes. This is a constrained system, and the results for  $\phi_{\text{shear}}(f_a)$  and  $\phi_{\text{bulk}}(f_a)$  for the five lowest frequency pairs of modes are shown in Table 4.

Uncertainties in  $\phi_{\text{shear}}(f_i)$  and  $\phi_{\text{bulk}}(f_i)$ ,  $\delta\phi_{\text{shear}}(f_i)$  and  $\delta\phi_{\text{bulk}}(f_i)$ , were determined from measurement uncertainties in  $\mathbf{q}$  and computational uncertainties in  $\mathbf{A}^{-1}$ . The uncertainty vector for the reciprocal Q's was found from

$$\delta \mathbf{q} = \begin{pmatrix} \delta Q_1/Q_1^2 \\ \delta Q_2/Q_2^2 \\ \vdots \\ \delta Q_n/Q_n^2, \end{pmatrix}$$
 (12)

where the  $\delta Q$ 's are from Table 1 and the uncertainties in  $\phi_{\rm silica}(f)$  are assumed

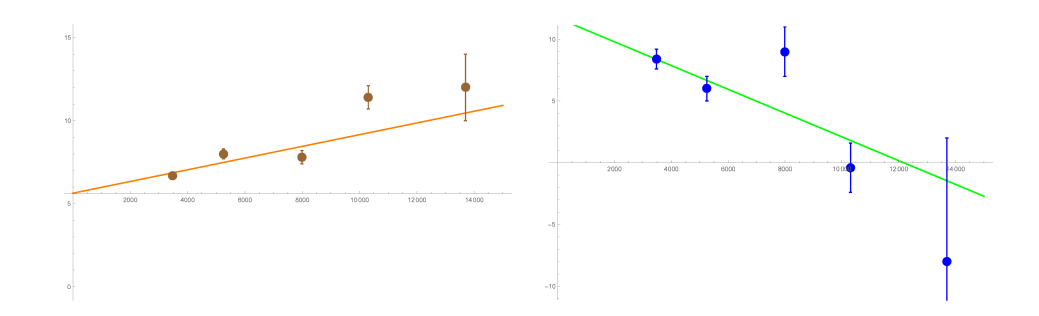


Figure 2: Mechanical loss as a function of frequency, showing  $\phi_{\text{shear}}$  on the left and  $\phi_{\text{bulk}}$  on the right.

to be negligible. Uncertainties in the matrix elements of  $\mathbf{A}^{-1}(=a_{k,\ell})$ 

$$\delta a_{k,\ell}^2 = \sum_{k=1,\ell=1}^{2,2} \left( \frac{\partial a_{i,j}}{\partial A_{k,\ell}} \delta A_{k,\ell} \right)^2 \tag{13}$$

The data in Table 4 is shown in Figure 3.1 as  $\phi_{\text{shear}}(f) \pm \delta\phi_{\text{shear}}(f)$  and  $\phi_{\text{bulk}}(f) \pm \delta\phi_{\text{bulk}}(f)$  versus frequency f. If the data is fit to a model with linear frequency dependence, which was used in [36], using the uncertainties as weights, the results are

$$\phi_{\text{shear}}(f) = (5.1 \pm 0.8) \times 10^{-4} + (4.7 \pm 1.5) \times 10^{-8} f,$$
 (14)

$$\phi_{\text{bulk}}(f) = (11 \pm 2) \times 10^{-4} - (8.3 \pm 4.6) \times 10^{-8} f.$$
 (15)

The  $\phi$  values in Table 4 fit to a constant model yield

$$\phi_{\text{shear}} = (7.4 \pm 0.6) \times 10^{-4}$$
 (16)

$$\phi_{\text{bulk}} = (7.2 \pm 1.0) \times 10^{-4}.$$
 (17)

The simple linear model of Equations 14 and 15 shown in Figure 3.1 cannot be consistent throughout the entire frequency range, otherwise, the bulk loss angle,  $\phi_{\text{bulk}}$ , would eventually reach negative values at frequencies above about 13 kHz. Materials typically exhibit more complex frequency dependence such as Debye loss peaks [37].

It has been found previously that tantala coatings made by CSIRO have had higher mechanical loss [38] than those coated by Laboratoire des Matériaux Avancés (LMA), the vendor that coated the Advanced LIGO, Advanced Virgo, and KAGRA optics [39]. It is suspected that some proprietary details of the ion beam deposition process that differ between vendors do have an impact on mechanical loss, although this is difficult to study. It is also known that post deposition annealing generally reduces mechanical loss [28]. The relatively high values for the loss angles in Equations 14- 17 compared to 25% titania doped

tantala coated by LMA [10] are consistent with both these vendor and annealing trends.

The finite element model shows modes near 37.0 and 41.5 kHz with almost the entire elastic energy due to shear deformation. We found these modes in our sample at 37013 Hz and 41521 Hz. These modes are listed in Tables 1 and 3 as modes 14 and 16. Following the analysis beginning with Equation 11 using these two modes we find shear and bulk loss angles of

$$\phi_{\text{shear}} (39267 \text{ Hz}) = (1.6 \pm 0.2) \times 10^{-7},$$
 (18)

$$\phi_{\text{bulk}} (39267 \text{ Hz}) = (4.1 \pm 0.1) \times 10^{-6},$$
 (19)

compared to

$$\phi_{\text{shear}} (39267 \text{ Hz}) = -2.5 \times 10^{-4},$$
 (20)

$$\phi_{\text{bulk}} (39267 \text{ Hz}) = 2.6 \times 10^{-4},$$
 (21)

predicted by Equations 14 and 15. These values indicate that the true frequency dependence of  $\phi_{\rm shear}$  and  $\phi_{\rm bulk}$  is more complicated than a simple linear model.

### 4. Applications

The paper by Hong et al. [18] characterizes the impact of the separate  $\phi_{\text{bulk}}(f)$  and  $\phi_{\text{shear}}(f)$  in terms of the ratio

$$r = \phi_{\text{bulk}}(f) / \phi_{\text{shear}}(f) \tag{22}$$

with lower values of r leading to lower coating Brownian thermal noise in the Advanced LIGO detectors. The constant values for the two loss angles from Equations (16) and (17) gives a value of

$$r = 1.1 \pm 0.8,\tag{23}$$

consistent with the value of r = 1 that is tacitly assumed in the Advanced LIGO noise model [5].

Using the frequency dependent forms of  $\phi_{\text{bulk}}(f)$  and  $\phi_{\text{shear}}(f)$  from Equations (14) and (15) gives

$$r(f) = \frac{(1.3 \pm 0.2) \times 10^{-4} - (9.8 \pm 4.7) \times 10^{-9} f}{(5.2 \pm 1.1) \times 10^{-5} + (5.4 \pm 2.1) \times 10^{-9} f},$$
(24)

with a value of

$$r(100 \text{ Hz}) = 2.6 \pm 1.8$$
 (25)

in the middle of the coating thermal noise limited frequency band of Advanced LIGO.

The test mass mirrors in the Advanced LIGO detectors [5] are made of a multi-layer stack of silica  $(SiO_2)$  and titania-doped tantala  $(Ti:Ta_2O_5)$  layers in a configuration that has been optimized to both reduce the added Brownian

thermal noise due to the higher mechanical loss of Ti:Ta<sub>2</sub>O<sub>5</sub> over SiO<sub>2</sub>, as well as to optimize reflectance at the infrared and green laser frequencies utilized in the detector [40]. A full analysis of the effects of the  $\phi_{\rm bulk}/\phi_{\rm shear}$  ratios measured here would require utilizing the full layer structure, as well as an equivalent measurement of the  $\phi_{\rm bulk}/\phi_{\rm shear}$  ratio for silica thin film. These are both topics of ongoing investigations.

However, Figures 8 and 9 from Hong et al [18] show the effects of varying  $\phi_{\text{bulk}}/\phi_{\text{shear}}$  ratios of silica and undoped tantala in a similarly-optimized coating. From these Figures, one can extract

- 1. The  $\phi_{\text{bulk}}/\phi_{\text{shear}}$  ratio of silica has a much smaller effect than that of tantala, due to its smaller elastic moduli and lower overall mechanical loss
- 2. Increasing only the  $\phi_{\rm bulk}/\phi_{\rm shear}$  ratio of tantala while keeping the ratio for silica at 1 leads to an increase in the Brownian thermal noise in the detector of about 18% for a tantala  $\phi_{\rm bulk}/\phi_{\rm shear}$  ratio of 2.6.
- 3. It may be possible to further optimize coatings such that this increase is mitigated, if it is found that silica has a ratio  $\phi_{\text{bulk}}/\phi_{\text{shear}} < 1$ . However, as the ratio for silica is reduced, it has an asymptote at only about 4% reduction.

Work recently published by Evans et al. [41] shows that the Brownian thermal noise measured directly in a cavity using an Advanced LIGO  $\rm SiO_2/Ti:Ta_2O_5$  coating has noise approximately 22% higher than the Advanced LIGO noise model [5]. This discrepancy is roughly the same as the 18% predicted by Hong et al. [18] with our extrapolated 100 Hz ratio, and may indicate that this will place a higher limit on the ultimate sensitivity of Advanced LIGO in its most sensitive frequencies.

In optical stabilization applications, the relevant frequency range can be as low as 10 mHz [2]. Using Equation (24) for such a low frequency also gives a value of  $r(10^{-3} \text{ Hz}) = 2.6 \pm 1.8$ , and results in similar offsets in the calculation of linewidth-limiting thermal noise.

There is ongoing work on whether common treatments such as doping and heat-treatment [42] can change the  $\phi_{\text{bulk}}\left(f\right)/\phi_{\text{shear}}\left(f\right)$  ratio in materials, or whether this ratio might be affected by the coating-substrate interface. Our work indicates that careful studies of materials under consideration for use in precision optical measurement must have their  $\phi_{\text{bulk}}\left(f\right)$  and  $\phi_{\text{shear}}\left(f\right)$  characterized, so that any gains made in total loss are not undone by an unfavorable ratio. It may even be possible to find low and high-index materials with ratios < 1 that would improve the Brownian noise below the level suggested by total loss measurements.

A complete understanding of the opportunities to improve coating Brownian thermal noise in future ground-based gravitational wave interferometers requires further meaurements of  $\phi_{\rm shear}$  and  $\phi_{\rm bulk}$  on titania-doped tantala, and other high index, thin films from other coating vendors, especially LMA. Shear and bulk losses on thin film silica and other low index materials are also necessary. This technique of analyzing modal Q results in terms of the imaginary components of

individual elastic constants will also prove valuable when careful predictions of coating thermal noise from crystalline coatings, like aluminum-gallium-arsenide (AlGaAs) [1] are necessary for third generation interferometeric gravitational wave detectors [43]. AlGaAs has the zinc blende symmetry system and has three independent elastic constants, making it more complicated to analyze than amorphuous materials with only two elastic constants.

### Acknowledgments

This work was supported by US National Science Foundation awards 1453252 and 1205481. We thank Ting Hong and Yanbei Chen for useful discussions. This paper has been assigned LIGO document number P1700093.

- [1] Garrett D. Cole, Wei Zhang, Michael J. Martin, Jun Ye, and Markus Aspelmeyer. Tenfold reduction of brownian noise in high-reflectivity optical coatings. *Nat Photon*, 7(8):644–650, Aug 2013. Article.
- [2] Kenji Numata, Amy Kemery, and Jordan Camp. Thermal-noise limit in the frequency stabilization of lasers with rigid cavities. *Physical Review Letters*, 93:250602, Dec 2004.
- [3] G Harry, TP Bodiya, and R DeSalvo. Optical Coatings and Thermal Noise in Precision Measurement. Optical Coatings and Thermal Noise in Precision Measurement. Cambridge University Press, 2012.
- [4] Gregory M Harry and the LIGO Scientific Collaboration. Advanced LIGO: the next generation of gravitational wave detectors. *Classical and Quantum Gravity*, 27(8):084006, 2010.
- [5] J. Aasi et al. (The LIGO Scientific Collaboration). Advanced LIGO. Classical and Quantum Gravity, 32(7):074001, 2015.
- [6] BS Sathyaprakash and BF Schutz. Physics, astrophysics and cosmology with gravitational waves. Living Reviews in Relativity, 12(2), 2009.
- [7] B. P. Abbott and et al. Observation of gravitational waves from a binary black hole merger. *Phys. Rev. Lett.*, 116:061102, Feb 2016.
- [8] B. P. Abbott and et al. Gw151226: Observation of gravitational waves from a 22-solar-mass binary black hole coalescence. *Phys. Rev. Lett.*, 116:241103, Jun 2016.
- [9] Steven D Penn, Peter H Sneddon, Helena Armandula, Joseph C Betzwieser, Gianpietro Cagnoli, Jordan Camp, D R M Crooks, Martin M Fejer, Andri M Gretarsson, Gregory M Harry, Jim Hough, Scott E Kittelberger, Michael J Mortonson, Roger Route, Sheila Rowan, and Christophoros C Vassiliou. Mechanical loss in tantala/silica dielectric mirror coatings. Classical and Quantum Gravity, 20(13):2917, 2003.

- [10] GM Harry, MR Abernathy, AE Becerra-Toledo, H Armandula, et al. Titania-doped tantala/silica coatings for gravitational-wave detection. Classical and Quantum Gravity, 24(2):405, 2007.
- [11] PR Saulson. Thermal noise in mechanical experiments. *Physical Review D*, 42:2437–2445, 1990.
- [12] Sheila Dwyer, Daniel Sigg, Stefan W. Ballmer, Lisa Barsotti, Nergis Mavalvala, and Matthew Evans. Gravitational wave detector with cosmological reach. *Phys. Rev. D*, 91:082001, Apr 2015.
- [13] G. M. Harry et al. Thermal noise in interferometric gravitational wave detectors due to dielectric optical coatings. *Classical and Quantum Gravity*, 19(5):897, 2002.
- [14] DRM Crooks, P Sneddon, G Cagnoli, J Hough, S Rowan, MM Fejer, E Gustafson, R Route, N Nakagawa, D Coyne, GM Harry, and AM Gretarsson. Excess mechanical loss associated with dielectric mirror coatings on test masses in interferometric gravitational wave detectors. *Classical* and Quantum Gravity, 19(5):883, 2002.
- [15] N Nakagawa, AM Gretarsson, EK Gustafson, and MM Fejer. Thermal noise in half-infinite mirrors with nonuniform loss: A slab of excess loss in a half-infinite mirror. *Physical Review D*, 65:102001, 2002.
- [16] Y Levin. Internal thermal noise in the LIGO test masses: A direct approach. *Physical Review D*, 57(2):659–663, 1998.
- [17] Callen HB and RF Greene. On the theorem of irreversible thermodynamics. *Physical Review*, 86:702–710, 1952.
- [18] Ting Hong, Huan Yang, Eric K. Gustafson, Rana X. Adhikari, and Yanbei Chen. Brownian thermal noise in multilayer coated mirrors. *Phys. Rev. D*, 87:082001, Apr 2013.
- [19] Andrew D. Ludlow, Martin M. Boyd, Jun Ye, E. Peik, and P. O. Schmidt. Optical atomic clocks. *Rev. Mod. Phys.*, 87:637–701, Jun 2015.
- [20] Hua Guan, Hu Shao, Yuan Qian, Yao Huang, Pei-Liang Liu, Wu Bian, Cheng-Bin Li, B. K. Sahoo, and Ke-Lin Gao. Combined experimental and theoretical probe of the lifetime of the  $3d^2D_{5/2}$  state in  $^{40}$ ca<sup>+</sup>. *Phys. Rev.* A, 91:022511, Feb 2015.
- [21] R. J. Rafac, B. C. Young, J. A. Beall, W. M. Itano, D. J. Wineland, and J. C. Bergquist. Sub-dekahertz ultraviolet spectroscopy of <sup>199</sup>hg<sup>+</sup>. *Phys. Rev. Lett.*, 85:2462–2465, Sep 2000.
- [22] B. C. Young, F. C. Cruz, W. M. Itano, and J. C. Bergquist. Visible lasers with subhertz linewidths. *Phys. Rev. Lett.*, 82:3799–3802, May 1999.

- [23] Mark Notcutt, Long-Sheng Ma, Andrew D. Ludlow, Seth M. Foreman, Jun Ye, and John L. Hall. Contribution of thermal noise to frequency stability of rigid optical cavity via hertz-linewidth lasers. *Phys. Rev. A*, 73:031804, Mar 2006.
- [24] Riccardo Bassiri, Matthew R. Abernathy, Franklin Liou, Apurva Mehta, Eric K. Gustafson, Martin J. Hart, Hafizah N. Isa, Namjun Kim, Angie C. Lin, Ian MacLaren, Iain W. Martin, Roger K. Route, Sheila Rowan, Badri Shyam, Jonathan F. Stebbins, and Martin M. Fejer. Order, disorder and mixing: The atomic structure of amorphous mixtures of titania and tantala. Journal of Non-Crystalline Solids, 438:59 66, 2016.
- [25] Martin J. Hart, Riccardo Bassiri, Konstantin B. Borisenko, Muriel Vron, Edgar F. Rauch, Iain W. Martin, Sheila Rowan, Martin M. Fejer, and Ian MacLaren. Medium range structural order in amorphous tantala spatially resolved with changes to atomic structure by thermal annealing. *Journal* of Non-Crystalline Solids, 438:10 – 17, 2016.
- [26] J. P. Trinastic, R. Hamdan, Y. Wu, L. Zhang, and Hai-Ping Cheng. Unified interatomic potential and energy barrier distributions for amorphous oxides. *The Journal of Chemical Physics*, 139(15), 2013.
- [27] D. T. Wei and A. W. Louderback. Us patent 4,142,958: Method for fabricating multi-layer optical films, 1979.
- [28] RP Netterfield, M Gross, FN Baynes, KL Green, et al. Low mechanical loss coatings for LIGO optics: progress report. In M. L. Fulton and J. D. T. Kruschwitz, editors, Society of Photo-Optical Instrumentation Engineers (SPIE) Conference Series, volume 5870, pages 144–152, 2005.
- [29] Sophocles J. Orfanidis. Electromagnetic Waves and Antennas, 2008.
- [30] Corning hpfs 7979, 7980, 8655 fused silica. https://www.corning.com/media/worldwide/csm/documents/5bf092438c5546dfa9b08e423348317b.pdf, 2014.
- [31] W. C. Oliver and G. M. Pharr. Measurement of hardness and elastic modulus by instrumented indentation: Advances in understanding and refinements to methodology. *Journal of Materials Research*, 19(01):3, 2004.
- [32] WC Oliver and GM Pharr. An improved technique for determining hardness and elastic modulus using load and displacement sensing indentation experiments. *Journal of Materials Research*, 7(06):1564–1583, 1992.
- [33] A. Rar, H. Song, and G. M. Pharr. Assessment of new relation for the elastic compliance of a film-substrate system. MRS Online Proceedings Library, 695:L10.10.1, 2001.

- [34] E. Çetinörgü, B. Baloukas, O. Zabeida, J. E. Klemberg-Sapieha, and L. Martinu. Mechanical and thermoelastic characteristics of optical thin films deposited by dual ion beam sputtering. *Applied Optics*, 48(23):4536– 4544, 2009.
- [35] R Flaminio, J Franc, C Michel, N Morgado, L Pinard, and B Sassolas. A study of coating mechanical and optical losses in view of reducing mirror thermal noise in gravitational wave detectors. Classical and Quantum Gravity, 27(8):084030, 2010.
- [36] D R M Crooks, G Cagnoli, M M Fejer, G Harry, J Hough, B T Khuri-Yakub, S Penn, R Route, S Rowan, P H Sneddon, I O Wygant, and G G Yaralioglu. Experimental measurements of mechanical dissipation associated with dielectric coatings formed using sio<sub>2</sub>, ta<sub>2</sub> o<sub>5</sub> and al<sub>2</sub> o<sub>3</sub>. Classical and Quantum Gravity, 23(15):4953, 2006.
- [37] VB Braginsky, VP Mitrofanov, and VI Panov. Systems with Small Dissipation. University of Chicago Press, Chicago, IL, 1985.
- [38] Kazuhiro Yamamoto, Shinji Miyoki, Takashi Uchiyama, Hideki Ishitsuka, Masatake Ohashi, Kazuaki Kuroda, Takayuki Tomaru, Nobuaki Sato, Toshikazu Suzuki, Tomiyoshi Haruyama, Akira Yamamoto, Takakazu Shintomi, Kenji Numata, Koichi Waseda, Kazuhiko Ito, and Koji Watanabe. Measurement of the mechanical loss of a cooled reflective coating for gravitational wave detection. *Phys. Rev. D*, 74:022002, Jul 2006.
- [39] Gregory Harry and Garilynn Billingsley. Advanced Interferometric Gravitational-wave Detectors. World Scientific Book, 2017.
- [40] J. Agresti, G. Castaldi, R. DeSalvo, V. Galdi, V. Pierro, and I. M. Pinto. Optimized multilayer dielectric mirror coatings for gravitational wave interferometers. In *Proceedings of the SPIE*, volume 6286, page 628608, 2006.
- [41] S. Gras, H. Yu, W. Yam, D. Martynov, and M. Evans. Audio-band coating thermal noise measurement for advanced ligo with a multimode optical resonator. *Phys. Rev. D*, 95:022001, Jan 2017.
- [42] I. W. Martin, R. Bassiri, R. Nawrodt, M. M. Fejer, et al. Effect of heat treatment on mechanical dissipation in Ta<sub>2</sub>O<sub>5</sub> coatings. Classical and Quantum Gravity, 27(22):225020, 2010.
- [43] Jessica Steinlechner, Iain W Martin, Angus Bell, Garrett Cole, Jim Hough, Steven Penn, Sheila Rowan, and Sebastian Steinlechner. Mapping the optical absorption of a substrate-transferred crystalline algaas coating at 1.5 μm. Classical and Quantum Gravity, 32(10):105008, 2015.